# Polyurethanes From Tung Oil: Polymer Characterization and Composites

AQ1 **M.A. Mosiewicki, U. Casado, N.E. Marcovich, M.I. Aranguren**
*Institute of Materials Science and Technology (INTEMA), University of Mar del Plata-National Research Council (CONICET), Av. Juan B. Justo 4302, (7600) Mar del Plata, Argentina*

**A natural polyol was obtained from tung oil (TO) to be further used in the formulation of rigid polyurethane polymers. The synthesis of the polyol was carried out in two steps: first hydroxylation of the double bonds in the fatty acid chains of the unsaturated oil and then, alcoholysis of the hydroxylated oil with triethanolamine. The chemical analysis (titration, FTIR, $^1$H NMR) of the unmodified TO, the hydroxylated tung oil, and the alcoholized hydroxylated tung oil-based polyol indicates that the hydroxyl content increased significantly after the hydroxylation and alcoholysis reactions. The modified TO was subsequently used as the polyol component in the formulation of reinforced rigid polyurethanes. Wood flour (WF) and microcrystalline cellulose were the reinforcements chosen to be incorporated in these materials. Physical, thermal, and mechanical properties of the neat and reinforced polyurethanes were measured and analyzed. An excellent dispersion of the WF in the matrix, confirmed by scanning electron microscopy, was observed in the polyurethane reinforced with WF. This system also presented the highest modulus and strength. POLYM. ENG. SCI., 00:000–000, 2008. © 2008 Society of Plastics Engineers**

## INTRODUCTION

Polyurethane polymers can be used in different applications to offer a wide range of properties from those of flexible elastomers to rigid crosslinked polymers. Although the main polyols used for polyurethanes production are derived from the petroleum industry [1], the use of renewable natural products as an alternative source for raw materials has gained increased importance in both basic research and industrial production during the last years. Vegetable oils are abundant and widely available; they are relatively low cost materials and offer a priori the possibility of biodegradation. They consist of triglyceride molecules that are esters of glycerol and fatty acids, predominantly unsaturated fatty acids. These triglycerides present many reactive sites able to be reacted in order to obtain a product for the polymer industry [2].

Natural polyols can be obtained by chemical modification of the vegetable oils introducing hydroxyl groups in an unsaturated triglyceride by hydroxylation of carbon–carbon double bonds and/or by alcoholysis of the triglyceride to obtain mainly a monoglyceride [2, 3].

Tung oil (TO), also called china wood oil, is obtained from the seeds or nuts of the tung tree [4]. This oil is interesting because its major constituent is α-eleostearic acid (77–82%) with three conjugated double bonds (at carbons 9 cis, 11 trans, 13 trans), whereas the other important components of TO are oleic acid (3.5–12.7%) with one double bond and linoleic acid (8–10%) with three nonconjugated double bonds [5, 6]. This characteristic makes it an excellent product to be used in the paint and varnish industry as drying oil because of its fast polymerization in presence of oxygen [7]. These multiple carbon–carbon double bonds are also capable to be reacted to introduce hydroxyl groups through a hydroxylation reaction.

On the other hand, the use of natural fibers as reinforcing material is an attractive alternative because they are obtained from renewable resources at relatively low costs compared to that of synthetic fibers [8]. Lignocellulosic fibers have high strength and modulus, so they can improve the mechanical properties of polymer composites and lower their costs. Additionally, vegetable fibers present surface hydroxyl groups that can interact chemically with the isocyanate group in the polyurethane, improving the fiber–matrix adhesion.

Although, polyurethane adhesives are widely used in different industries, not many works have reported on the use of oil-based polyols in polyurethane formulations and the study of these materials and their properties is still scarce.

The aim of this work is to synthesize and to characterize a polyol from TO to be used in the formulation of reinforced polyurethanes. The effect of the addition of natural fibers to the polymer on the thermal and mechanical properties will also be evaluated.

*Correspondence to*: M. I. Aranguren; e-mail: marangur@fi.mdp.edu.ar
Contract grant sponsors: CONICET, ANPCyT.
DOI 10.1002/pen.21300
Published online in Wiley InterScience (www.interscience.wiley.com).

## EXPERIMENTAL

### *Materials*

The natural polyol was obtained from TO (Cooperativa Agrícola Limitada de Picada Libertad, Argentina, saponification value = 223 mg KOH/g, acid number = 2.11 mg KOH/g). Hydrogen peroxide (30 wt%) and formic acid (88 wt%) from Laboratorios Cicarelli were used in the hydroxylation reaction. Triethanolamine (TEOA, >99%) from Laboratorios Cicarelli and lithium hydroxide (>99%) from Fluka were used in the alcoholysis reaction.

In the preparation of the polyurethane polymers, the isocyanate used was a commercial polymeric 4,4′-diphenylmethane diisocyanate, pMDI (Rubinate 5005, Huntsman Polyurethanes, USA) with an equivalent weight of 131 g/eq. Pine wood flour (WF, Jorge Do Santos Freire, Buenos Aires, Argentina) and microcrystalline cellulose (MCC, Avicel PH-101, FMC Biopolymer, Philadelphia, PA) were selected as the reinforcement/reactive fillers. WF had particle sizes $\leq$64 $\mu$m and the microcellulose consists of cellulose aggregates in the micron scale (largest aggregates are about 30–50 $\mu$m) [9].

Before using, WF, MCC, and polyol were dried until constant weight (70°C, vacuum oven).

The OH values of the WF and the MCC were determined using a back titration technique. A measured weight of WF was mixed with excess of pMDI. After the reaction was completed, the free NCO groups were determined according to the technique described elsewhere [10]. The resulting values were 233.3 mg KOH/g for the WF and 209.4 mg KOH/g for the MCC.

### *Synthesis of Tung Oil-Based Polyols*

**Hydroxylated Tung Oil.** Hydrogen peroxide solution and formic acid were added to a stirred reactor and the temperature was raised to 40°C. The oil was added dropwise and the temperature was kept between 40 and 50°C for 3 h. After that the final product was cooled down to room temperature. The liquid separated clearly in two phases. The upper layer was recovered and distilled under vacuum to eliminate remaining water and acid. In this first step of the synthesis, the initial ratios oil/$H_2O_2$ (weight) = 3.5/1 and $H_2O_2$/HCOOH (weight) = 1/1.9 were utilized.

During this step, the hydrogen peroxide reacts with the formic acid to form performic acid. After the TO is incorporated, it undergoes an intermediate process of epoxidation. The epoxide group is unstable under the strong acid conditions and it opens to form hydroxyl groups [3].

**Alcoholysed Hydroxilated Tung Oil.** The hydroxylated tung oil (HTO), dry TEOA, and lithium hydroxide (catalyst) were added together in a reactor with mechanical stirrer. The temperature was raised to 150°C in 0.5 h and further kept at this value for 2.5 h. The HTO/TEOA weight ratio was of 2/1 and the catalyst was added as a 0.2 wt% of the total reactants. This is a complex step of reaction consisting mainly in a transesterification of the triglyceride molecules with the ethanol moieties of the TEOA. The final products are a mixture of different polyalcohols containing one or two hydroxylated fatty acid chains.

### *Preparation of the Polyurethane and Composites*

The TO-derived polyol was dried (at 60°C under vacuum and gentle stirring) and stored. To formulate the PU, the dried polyol was dissolved in tetrahydrofuran (THF) in order to decrease the initial viscosity and reduce the reaction rate. The molar ratio NCO groups/OH groups used in the production of the polyurethanes reinforced with WF or MCC was 1.10 (the excess was added to account for any remaining absorbed moisture in the dried reactants). After adding the pMDI (or the pMDI and the filler, for reinforced polyurethanes), the system was mechanically mixed for 20 s and then the reactive mixture was put in a metal mold of 14 cm of internal diameter. The THF was allowed to evaporate in the open mold and then the mold was closed and the samples were cured at 75°C under a pressure of 4 MPa, obtaining 1-mm-thick plates. Samples of 10 wt% of MCC and 10 wt% of WF were molded according this procedure.

### *Physical-Chemical Characterization of the Materials*

The viscosity of the TO was measured at room temperature using a Brookfield DV-II and CPE-40 spindle.

The original oil and derived precursors were characterized using analytical techniques (hydroxyl value, acid number, and saponification values) [11].

Transmission infrared spectroscopy, FTIR, was also utilized in the chemical characterization of the initial oil and later modifications, using smeared samples on NaCl windows. All spectra were recorded at 2 $cm^{-1}$ resolution with the use of a Genesis II Fourier transform infrared spectrometer. Results reported were the average of 16 scans.

The TO and the alcoholized tung oil were characterized by $^1$H NMR (Bruker AM-500 spectrometer), using deuterated acetone and deuterated dimethylsulfoxide as solvents, respectively.

Size exclusion chromatography (SEC) was used to follow the distribution of molecular weights in the initial oil and in the products obtained from the two steps of the polyol synthesis. A set of glass tubes containing known masses of a given sample (8–25 mg) were dissolved in 5 mL of THF. Injections of 10 $\mu$L of the resulting solutions were analyzed by size exclusion chromatography (SEC, Knauer K-501, RI detector Knauer K-2301, and a set of Phenomenex Phenogel 5 $\mu$-columns: 50A, 100A, and M2), using THF as the carrier at 1 $cm^3$/min.


DOI 10.1002/pen

TABLE 1. Analytical characterization of the tung oil and modified tung oil.

| | Tung oil | Hydroxylated tung oil | Tung oil-based polyol |
|---|---|---|---|
| Hydroxyl value (mg KOH/g) | 0 | 287 | 434.0 |
| Acid number (mg NaOH/g) | 2.6 | n.d. | 53.1 |
| Saponification value (mg KOH/g) | 187.4 | n.d. | 190.4 |

n.d., not determined.

**Dynamic-Mechanical Tests.** Dynamic-mechanical tests were performed in a Perkin Elmer dynamic mechanical analyzer, DMA 7e, using tensile fixtures under nitrogen atmosphere. The specimens were cut to 20 mm × 4 mm × 1 mm, linear dimensions, measured ±0.01 mm. The dynamic and static stresses were kept at 200 and 240 kPa, respectively. The frequency of the forced oscillations was fixed at 1 Hz and the heating rate was of 10°C/min. At least two replicate determinations were made for each sample to ensure the reproducibility of results.

**Tensile Tests.** Specimens of each sample were cut and tested at room temperature and at a crosshead speed of 1 mm/min in an INSTRON 8501 Universal testing machine, according to the ASTM D638-94. At least four specimens of each sample were tested, and the average values and standard deviations were calculated.

**Microscopy of Fractured Specimens.** Scanning electron microscopy (SEM) was used to obtain photographs of the surfaces of the composites tested and fractured in tensile mode (scanning electron microscope Philips model SEM 505). Specimens were coated with gold previously to the microscopy observation.

**Thermogravimetric Analysis.** Thermogravimetric tests were performed in the 30–500°C range, using a TGA-50 SHIMADZU Thermogravimetric Analyzer at a heating speed of 10°C/min under nitrogen atmosphere.

## RESULTS AND DISCUSSION

### *Characterization of the Tung Oil and Its Modifications*

TO is a light brown liquid with a viscosity of 397 m Pa s measured at 25°C. After the modification (first and second steps) the viscosity increases to reach a paste like consistency. This high viscosity results from the introduction of hydroxyl groups to the modified TO species and the corresponding intermolecular H-bond interactions that take place because of that. Consequently, the obtained polyol is a highly hydrophilic reactant.

Table 1 shows that the unmodified TO has essentially no OH groups and very little free acids. After the modification, the resulting polyol has a hydroxyl value of 434 mg KOH/g, which is in the range commonly used to obtain rigid polyurethanes. However, the acid value also increases as a result of the initial step of modification. Saponification values (which measure acid and ester groups) were determined and are also reported in Table 1. Analysis of the values obtained indicated that the initial oil has three ester groups per 914.4 g of sample ($3.28 \times 10^{-3}$ mol/g). Notice that this is the estimated molar mass if the triglyceride molecules are essentially monodisperse.

**Molecular Weight.** The distribution of products with different molecular weights in the TO and derived polyol were compared using a polystyrene standard calibration. Figure 1 shows the comparison between the chromatograms obtained from size exclusion chromatography (SEC) for TO (curve A), HTO (curve B), and alcoholized hydroxylated tung oil (AHTO) (curve C).

The TO chromatogram consists essentially of a single peak corresponding to the triglyceride molecules, indicating that the glyceride composition is rather homogeneous in the oil, and so the material is practically monodisperse. The molar mass resulting from the use of a polystyrene standard calibration is 2110 g/mol. This value is clearly higher than the theoretically calculated value ($M_n$ = 875.4 g/mol) and also than the value calculated from the saponification acid numbers assuming that the oil is monodisperse ($M_n$ = 914.4 g/mol). John et al. [12] have previously reported a large aberration in the SEC characterization of triglycerides. They worked with soy oil and although the polydispersity of the samples was very low ($M_w/M_n$ = 1.01), as it is the case in this work, the molar masses determined by this method almost doubled the actual masses of the triglycerides. They reported that although the molecular weight of single fatty acids seems not to suffer aberration from using the PS calibration in the SEC measurements, triglyceride samples suffer this problem, resulting in the determination of much larger molar mass values than the theoretically expected values.

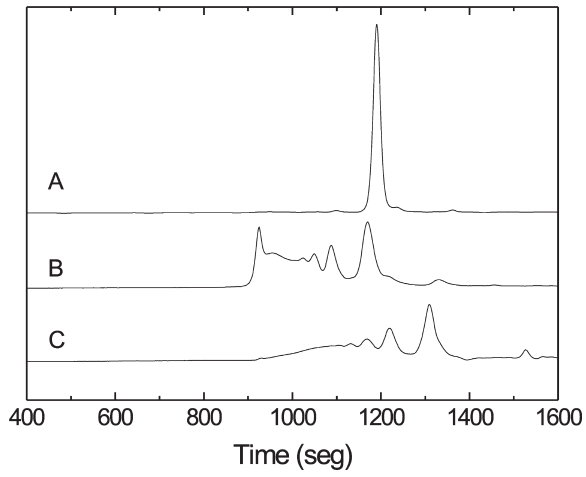


FIG. 1. SEC curves of TO (curve A), HTO (curve B), and AHTO (curve C).

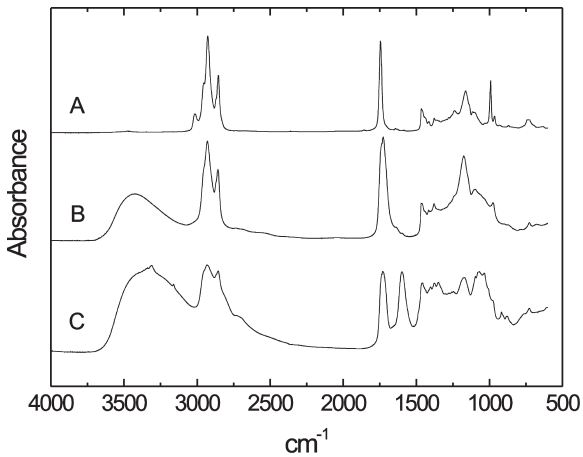


FIG. 2. FTIR spectra of TO (curve A), HTO (curve B), and AHTO (curve C).

The proposed reason for this effect was the difference between the linear molecular structure of PS and the three arms—molecular structure of the triglyceride molecules.

The chromatogram corresponding to the HTO shows lower retention volumes and wider peaks compared to TO without chemical modification. Although the retention times indicate the right expected trend of increasing molecular weight and the probable appearance of oligomeric species at this step (association of molecules through strong H-bonding), the absolute molecular weights suffer from the same aberration already described.

In the chromatogram corresponding to AHTO the effect is less important due to the decrease in molecular weight of this product. There is still a large contribution from high molecular weight species.

F2 **FTIR Characterization.** Figure 2 shows the comparison of the spectra of the unmodified and modified TO by hydroxylation first and alcoholysis later (curves A, B, and C, respectively). The FTIR spectrum of the TO (curve A) shows a negligible absorption at 3400–3500 $cm^{-1}$ in agreement with the chemical analysis of OH groups. The peak at 3010 $cm^{-1}$ corresponding to unsaturations is clearly observed. The peak at 1745 $cm^{-1}$ corresponds to the ester groups from triglyceride molecules and there is a small peak at 1643 $cm^{-1}$ that is assigned to the absorption of the double bonds in cis conformation. The existence of peaks at 965 and 735 $cm^{-1}$ indicates that both cis and trans conformations are present in the fatty acids that form the triglyceride. There is a rather high peak at 991 $cm^{-1}$ that corresponds to the wag of the conjugated unsaturations of the elaeostearic chains.

The most important difference among the curves is the increase in the band intensity at 3450 $cm^{-1}$ after the hydroxylation and alcoholysis reactions, corresponding to hydroxyl absorption, also related to the observed increase in the hydroxyl number of these samples. The spectra of the HTO shows a peak characteristic to secondary hydroxyl groups at 1098 $cm^{-1}$, and it is possible to observe the disappearance of the bands at 3010, 1640, and 991 $cm^{-1}$ corresponding to the carbon–carbon double bonds, which are present in the highly unsaturated TO (curve A) indicating that unsaturations disappear after the functionalization process.

In the alcoholysis step (AHTO) different reactions can take place, which lead mainly to the breakage of the molecules to give species of lower molecular weight. The clearest change occurs in the 3300–3500 $cm^{-1}$ region. As already mentioned, the intensity of this band grows after the second step due to the increase of hydroxyl groups. Additionally, although the main reaction at this step is the transesterification between the HTO and TEOA, some secondary reactions also occur. This leads to the appearance of an absorption band at 1598 $cm^{-1}$, probably due to amide groups [3].

In spectra (B) and (C), the peak at 1720–1745 $cm^{-1}$ appears broader than the peak at 1745 $cm^{-1}$ in the initial TO, indicating that acid and ester groups are contributing to the total absorption in this region. As discussed before, the final polyol has a larger acid value than the initial triglyceride (Table 1).

**$^1$H NMR Characterization.** The $^1$H NMR was analyzed, taking as simplifying initial assumption that the main fatty acids present in the oil were elaeostearic and oleic acids. The assignment of the peaks are shown in Fig. 3 and the areas measured from the spectrum are presented in Table 2, taking as the basis that the area at 0.9 ppm corresponds to the nine H's of the methyl protons per triglyceride at the end of the three fatty acid chains. The two multiplets at 4.4 to 4.1 ppm corresponds to the four glycerol methylene protons in the triglyceride molecule, while the small multiplet at 5.3 ppm corresponds to

F3 T2

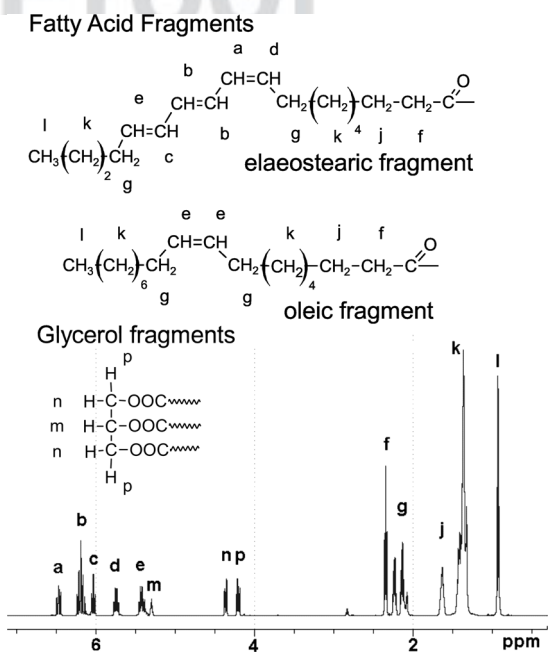


FIG. 3. $^1$H NMR corresponding to the unmodified TO.

TABLE 2. Measured and calculated areas in the spectra of $^1$H NMR of the unmodified tung oil (TO).

| | ppm | Theor. Oleic | Theor elaeostearic | Theor Triglyceride | Experimental |
|---|---|---|---|---|---|
| Fatty acid fragments | | | | | |
| a | 6.45 | — | 1 | 2.508 | 2.229 |
| b | 6.17 | | 2 | 5.016 | 4.732 |
| c | 6.0 | | 1 | 2.508 | 2.345 |
| d | 5.7 | | 1 | 2.508 | 2.364 |
| e | 5.4 | 2 | 1 | 3.492 | 3.388 |
| f | 2.3 | 2 | 2 | 6 | 5.823 |
| g | 2.05 | 4 | 4 | 12 | 11.542 |
| j | 1.6 | 2 | 2 | 6 | 5.967 |
| k | 1.43–1.16 | 20 | 12 | 39.936 | 39.936[a] |
| l | 0.9 | 3 | 3 | 9 | 9[b] |
| Glycerol fragment | | | | | |
| m | 5.29 | | | 1 | 0.938 |
| n | 4.34 | | | 2 | 1.871 |
| p | 4.15 | | | 2 | 1.878 |
| Total protons: | | | | 93.968 | 92.006 |

[a] The value of this peak was used to estimate the oleic and elaeostearic proportion in the triglyceride.
[b] Reference peak.

the central H in the glycerol moieties. The spectrum does not show any peak at 2.8 ppm, which indicates that there is no contribution of bis-allylic protons (—$CH_2$, comprised between two unsaturations). This indicates that there are essentially no linoleic or linolenic fatty acids in the composition of the triglyceride. This is also the reason to have chosen the simplified composition already indicated.

The peaks at 1.43–1.16 ppm correspond to the olefinic protons separated at least two carbons from the ester groups and at least one carbon from the unsaturations. Thus, in these peaks there are contributions from the elaeostearic and the oleic fatty acids considered in the structure. Since the contribution is different from each fatty acid, the percentage of each one can be calculated. This resulted in a 83.6% (molar) of elaeostearic acid and 16.4% (molar) of oleic acid. This result is in very good agreement with composition data for TO reported in the literature [5, 6, 13].

Once the proportion of fatty acids was estimated, the theoretical values of each of the areas assigned could be calculated. Table 2 shows the theoretically calculated and experimentally found values of the areas. As it can be seen and although the composition of the oil was rather simplified, the experimental and theoretical values are very much in agreement, which support the idea of a large concentration of the elaeostearic acid. Additionally, $^1$H NMR results agree with the SEC results as well as the analytical characterization; all of them indicating that the oil is essentially monodisperse and formed mainly by triglycerides containing elaeostearic acid.

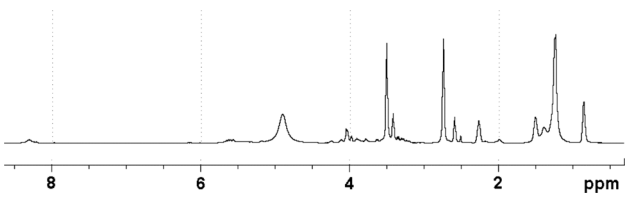


FIG. 4. $^1$H NMR corresponding to the AHTO.

The $^1$H NMR spectrum of the AHTO is shown in Fig. 4. The more clear changes with respect to the triglyceride are the disappearance of the peaks corresponding to protons in the unsaturations and the appearance of rather broad peak at 4.7−5.2 ppm corresponding to the hydroxyl protons. The small peak appearing above 8 ppm is assigned to protons in acid groups. F4

*Polyurethanes*

The polyurethanes prepared from the formulations indicated in the Materials section were rigid materials of light brown color, since the polyol and the polymeric pMDI utilized in the formulation are brown in color. The polymeric matrix shows no visible bubbles.

**Dynamical-Mechanical Analysis.** The polyurethane samples were tested in tensile dynamic mode and representative curves of the storage modulus, $E'$, and tan $\delta$ are shown in Fig. 5. The room temperature storage modulus F5

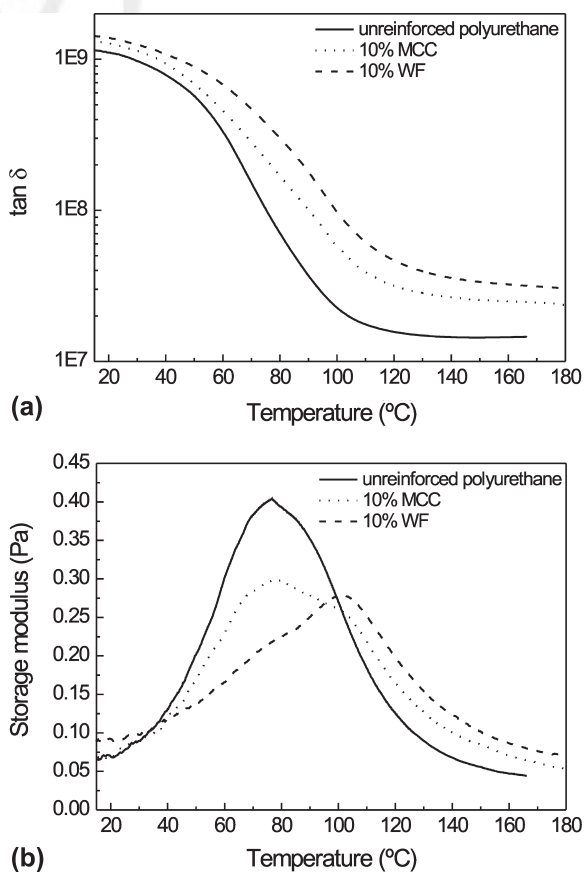


FIG. 5. Dynamic mechanical curves for unreinforced polyurethane and reinforced polyurethane with 10 wt% MCC and 10 wt% WF. (a) $E'$ versus temperature, (b) tan $\delta$.

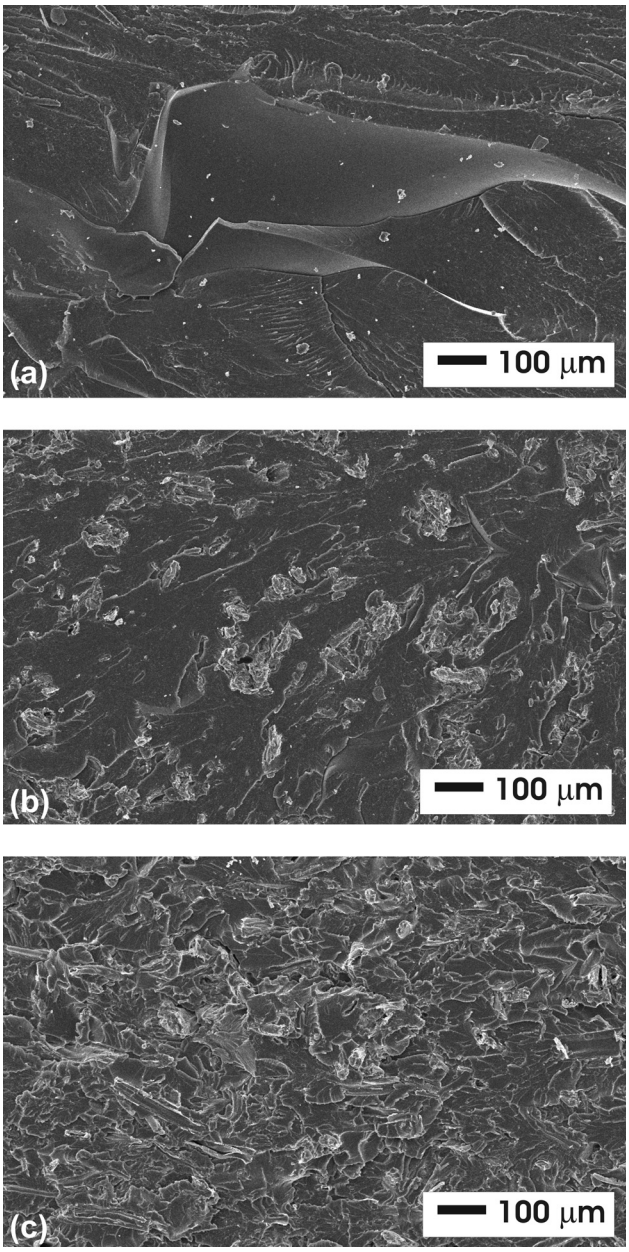


FIG. 6. Micrographs obtained by SEM. (a) unreinforced polyurethane, (b) polyurethane reinforced with 10 wt% MCC, (c) polyurethane reinforced with 10 wt% WF.

(1.2 GPa) decreases rapidly as temperature increases, entering the transition to the rubber region; at 30°C the modulus is already about 1 GPa. The transition region is very wide in this material, covering from nearly 20 to 140°C, showing the maximum at 77°C. The position of this maximum is related to the glass transition temperature, $T_g$, of the material. Finally, the drop in the $E'$ is such that the rubbery modulus becomes 14 MPa above 120°C.

**Mechanical Properties and Fracture Surface Morphology.** The quasi-static tensile mechanical properties of the rigid polyurethanes formulated with the natural polyol (AHTO) without reinforcements resulted in a Young modulus of 0.91 ± 0.12 GPa (in good agreement with the dynamic value already discussed), tensile stress of 26.00 ± 2.56 MPa, and tensile ultimate deformation of 3.45% ± 0.18%.

After fracture, the tensile specimens were observed by scanning electron microscopy (Fig. 6a). It was noticed that the samples were not foamed (efficient drying of the polyol was performed before sample preparation). Additionally, the fracture surfaces showed some plastic deformation, which was the result of the relatively low $T_g$ of the material.

**Thermal Stability.** The thermal stability of the unreinforced natural polyurethane was examined by TGA and the curve of weight loss versus temperature is shown in Fig. 7.

The corresponding curve to unreinforced polyurethane presents mainly two degradation steps. The first step starts at about 200°C and is associated with the ruptured of urethane links [14, 15]. The second step at temperatures higher than 400°C can be attributed to the polyol decomposition.

*Polyurethane Composites*

The potential for using these polyurethanes in the preparation of vegetable filler composites was also considered. For this reason, composites reinforced with WF and with MCC (at 10 wt% concentration) were prepared and characterized. Both fillers were easily dispersed in the initial reactants, however although no WF aggregation was noticeable (by naked eye), some added turbidity was visible in the MCC composites.

**Dynamic Mechanical Analysis.** Figure 5a and b show the temperature dependence of the storage modulus and tan $\delta$ for the unreinforced polyurethane and reinforced polyurethanes with 10 wt% of MCC and 10 wt% of WF.

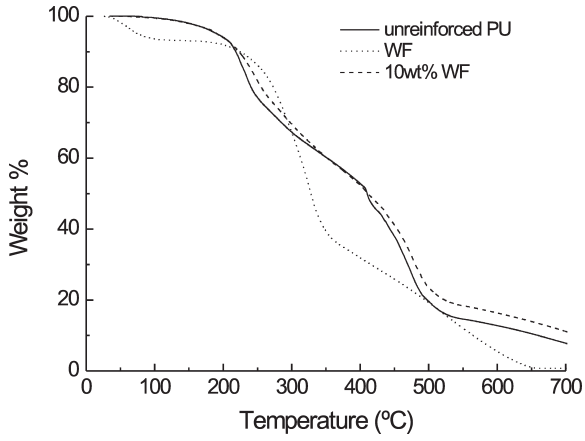


FIG. 7. TGA curves of unreinforced polyurethane, MCC, WF, and reinforced polyurethane with 10 wt% of MCC and 10 wt% of WF.


DOI 10.1002/pen

TABLE 3. Tensile results of unreinforced polyurethane and reinforced polyurethane with 10 wt% MCC and 10 wt% WF.

| | Tensile modulus (GPa) | Tensile strength (MPa) | Tensile ultimate deformation (×1000) |
|---|---|---|---|
| 0% WF | 0.91 ± 0.12 | 26.00 ± 2.56 | 34.5 ± 1.8 |
| 10% WF | 1.23 ± 0.13 | 35.65 ± 1.75 | 45.9 ± 3.5 |
| 10% MCC | 1.02 ± 0.03 | 24.91 ± 1.53 | 39.9 ± 3.8 |

Addition of any of the fillers increases the modulus of the polyurethane. However, WF increases in 25 and 96% the $E'$ in the room temperature and rubbery regions (at 160°C), respectively. The effect of addition of MCC is limited to 14 and 42% increase in the same conditions. As expected, at temperatures above $\alpha$ transition, the $E'$ enhancement is more important due to the larger difference between the modulus of the rigid filler particles and the rubbery modulus of the matrix.

The analysis of the tan $\delta$ curves shows that the peaks of the composites have lower height as compared to the neat polymer and also that the extent of the transition region is even wider. Both fillers present free hydroxyl groups able to interact chemically with the pMDI and to originate new bonds, chemically linking the matrix and the reinforcement. The reduced height of the peak after WF addition indicates that the presence of filler reduces the composite's ability to dissipate mechanical energy, that is, it reduces the damping capability.

It is also interesting to notice that the transition peak has at least two main contributions, one centered at 77°C as in the case of the unfilled polymer, and other centered around 100°C. The low temperature contribution is related to the relaxation of the unmodified polyurethane network, but it is proposed that the higher temperature contribution is related to the network modified/reacted with the OH containing fillers. It is interesting to observe that the WF composite has a larger contribution to the transition in the high temperature range, while the opposite is true for the MC composite. This would indicate a larger interaction/bonding between the WF and the polymer than that occurring for MC. This interpretation is supported by the higher modulus of the WF composite.

T3 Table 3 reports the mechanical properties of the reinforced polyurethane with 10 wt% of WF and another with 10 wt% of MCC as well as the neat polyurethane for easier comparison. The MCC composite presents less modulus and strength values than the WF composite at the same weigh percentage of filler. The better particle dispersion in the WF-reinforced polyurethanes, already mentioned, is suggested as one of the reasons for higher properties of this material, as it will be further discussed.

In composite materials, the strength is determined by that of the reinforcement and matrix and also by the ability of this matrix to transmit stress to the reinforcement [16]. If the particles are forming agglomerates in the composite, the transmission of stress is affected and the strength of the material is reduced. The formation of agglomerates is observed by SEM and this can be the reason of less ultimate stress in MCC reinforced polyurethane.

When the filler–matrix adhesion is adequate, the particles/fibers act as reinforcement in the matrix. This is the case of composite material reinforced with WF, which shows increase in modulus and strength with respect to the unfilled polyurethane. In the material containing MCC, the adhesion is good (confirmed by SEM) but the bad dispersion of MCC particles leads to the decrease in properties with respect to the matrix. The MCC acts as filler in the matrix.

Figure 6 shows the fracture surface of the composites formulated with the natural polyol (AHTO) containing 10 wt% of MC (Fig. 6b) or 10%wt of WF (Fig. 6c). The surfaces of the reinforced materials are substantially more irregular than the fracture surface of the neat polyurethane, and the WF composite surface is rougher than that of the MCC composite. The material containing MCC seems to present agglomeration of particles. The poorer dispersion on the system with MCC is originated in the fact that MCC is formed by the aggregation of a large number of individual crystallites strongly interassociated through hydrogen bonds [17]. Thus, it results more difficult to separate and to disperse MCC in the polymer. The presence of other components in WF, besides cellulose, may also account for the better ease of its dispersion in the matrix. In spite of this, the micrographic view of the interfacial region shows good interfacial adhesion on both systems.

The SEM observation is in agreement with the DMA analysis, that is, a stronger (or a larger concentration) of matrix reinforcement bonding appears to happens in the WF composite as compared to the MC composite. The same reasoning can be applied to the tensile mechanical results.

The thermal stability of the unreinforced natural polyurethane and the reinforced polyurethanes with 10 wt% of WF and 10 wt% of MCC was examined by TGA and the curves obtained of loss weight versus temperature are shown in Fig. 7. The curves corresponding to MCC and WF show that at temperatures below 150°C the absorbed moisture is lost. The MCC and WF have a hydrophilic nature able to interact with room moisture. While MCC presents a single degradation step (since it is essentially pure cellulose) at about 320°C, WF has a more complex degradation pattern, which is the result of the many and interacting components in its structure. MCC and WF leave no residue after 600 and 700°C, respectively.

The two reinforced polyurethanes present similar curves to that of the neat crosslinked polymer. However, at temperatures above 200°C, both reinforced polyurethanes present higher residual mass than the neat polyurethane. The additional reaction between pMDI and the hydroxyl groups in the MCC or WF originates new bonds, which give higher thermal stability to the composite materials.

## CONCLUSIONS

TO can be modified (hydroxylation and posterior alcoholysis) to obtain a polyol with a hydroxyl value high enough to be used in the formulation of rigid polyurethanes. The characterization of the polyols allowed identifying the changes produced in each reaction step. The analysis showed the disappearance of the unsaturations in the triglyceride and the increase of the OH concentration in the modified polyol as compared to the initial oil.

Vegetable-based fillers resulted to be appropriate fillers for rigid polyurethanes. MCC and WF were easily wet by the polyurethane precursors, due to specific H-bonds as well as chemical reaction between cellulosic OH and isocyanate groups, which leads to a good matrix–fiber adhesion in the composite material. The dispersion of particles into the polymer is worse in the system reinforced with MCC because of the agglomeration of crystalline particles, thus this system presents lower mechanical and dynamic-mechanical properties. The MCC acts mostly as filler, while the WF reinforces the material. Additionally, incorporating the fillers into the polymer improves the thermal stability of the composites at high temperatures.

## ACKNOWLEDGMENTS

The authors thank Mr. Oscar Casemayor for chemical analytical measurements.

## REFERENCES

1. K.S. Chian and L.H. Gan, *J. Appl. Polym. Sci.*, **68**, 509 (1998).
2. S.N. Khot, J.J. Lascala, E. Can, S.S. Morye, G.I. Williams, G.R. Palmese, S.H. Kusefoglu, and R.P. Wool, *J. Appl. Polym. Sci.*, **82**, 703 (2001).
3. Y.H. Hu, Y. Gao, D.N. Wang, C.P. Hu, S. Zhu, L. Vanoverloop, and D. Randall, *J. Appl. Polym. Sci.*, **84**, 591 (2002).
4. E. C. Wood, *Tung Oil: A New American Industry*, U.S. Government Printing Office, Washington, DC (1949).
5. M. W. Formo, E. Jungermann, F. A. Norris, and N.O. V. Sonntag, in *Bailey's Industrial Oil and Fat Products*, **Vol. 1**, 4th ed., D. Swern, Ed., Wiley, New York (1985). AQ2
6. X. Kong and S. S. Narine, "Industrial and Consumer Nonedible Products from Oils and Fats," in *Vegetable Oils in Production of Polymers and Plastics*, **Vol. 6**, F. Shahidi, Ed., Wiley, New York, Chapter 8, 279 (2005).
7. R. G. Kinabrew, *Tung Oil in Mississippi, The Competitive Position of the Industry*, University of Mississippi, Mississippi (1952).
8. N.E. Marcovich, M.M. Reboredo, and M.I. Aranguren, *J. Appl. Polym. Sci.*, **70**, 2121 (1998).
9. N.E. Marcovich, N.E. Bellesi, M.I. Aranguren, M.L. Auad, and S.R. Nutt, *J. Mater. Res.*, **21**, 870 (2006).
10. J. Urbanski, "Polyurethanes" in *Handbook of Analysis of Synthetic Polymers and Plastics*, J. Urbanski, W. Czerwinski, K. Janicka, F. Majewska, and H. Zowall, Eds., Wiley, Polonia, Chapter 11, Section: 11.2 Quantitative Analysis, 328 (1977).
11. J. Urbanski, "Chemical Methods" in *Handbook of Analysis of Synthetic Polymers and Plastics*, J. Urbanski, W. Czerwinski, K. Janicka, F. Majewska, and H. Zowall, Eds., Wiley, Polonia, Chapter 1, Section 1.2: Estimation of Chemical Characteristics, 48 (1977).
12. J. John, M. Bhattacharya, and R.B. Turner, *J. Appl. Polym. Sci.*, **86**, 3097 (2002).
13. F. Li and R. C. Larock, *J. Appl. Polym. Sci.*, **78**(5), 1044 (2000).
14. N. H. G. Jellinek and S. R. Dankle, *Degradation and Stability of Polymers*, Elsevier, London, 91 (1983).
15. D. J. David and M. P. Staley, *Analytical Chemistry of Polyurethane, Part III: High Polymers*, **Vol. XXI**, Wiley Interscience, New York, 365 (1974).
16. P. A. Peltola, In *Green Composites*, C. Baillie, Ed., CRC Press, Boca Raton, Chapter 5, 90 (2004).
17. A. P. Matheu, K. Oksman, and M. Sain, *J. Appl. Polym. Sci.*, **97**(5), 2014 (2005).